

Combustion-Transition Interaction in a Jet Flame

A. J. Yule,* N. A. Chigier,† S. Ralph,‡ R. Boulderstone,§ and J. Ventura§
University of Sheffield, Sheffield, England

The transition between laminar and turbulent flow in a round jet flame is studied experimentally. Comparison is made between transition in nonburning and burning jets and between jet flames with systematic variation in initial Reynolds number and equivalence ratio. Measurements are made using laser anemometry, miniature thermocouples, ionization probes, laser Schlieren, and high-speed cine films. Compared with the cold jet, the jet flame has a longer potential core, undergoes a slower transition to turbulence, has lower values of fluctuating velocity near the burner with higher values further downstream, and contains higher velocity gradients in the mixing layer region although the total jet width does not alter greatly in the first twenty diameters. As in the cold jet, transitional flow in the flame contains waves and vortices and these convolute and stretch the initially laminar interface burning region. Unlike the cold jet, which has Kelvin-Helmholtz instabilities, the jet flame can contain at least two initial instabilities: an inner high-frequency, combustion-driven instability and an outer, low-frequency instability that may be influenced by buoyancy forces.

Introduction

THE objective of this research is to obtain increased understanding of turbulent combustion in flows related to propulsion systems. Measurement and data analysis techniques, and the boundary conditions of the flames, are designed to provide an improved conceptual framework and fundamental experimental data to aid the development and checking of modeling techniques for practical combustion systems. Fundamental information and insight are required on the "physics" of reacting flows and this information must be sufficiently extensive and accurate to be of use to those involved in attempting to model and predict turbulent combustion. The measurements reported herein concentrate on the initial region of gaseous jet flames with separate variation in Reynolds number and equivalence ratio. These measurements have produced interesting and detailed data that are of potential use to combustion modeling groups, particularly because of the carefully controlled and measured initial and boundary conditions of the flames.

In recent years there have been several investigations of axisymmetric, nonreacting turbulent jets developing from laminar nozzle boundary layers. Yule¹ described how the transitional mixing layer contains vortex rings which gradually develop azimuthal core waves. Turbulent flow is established when these distorted vortex rings coalesce. The turbulent mixing layer and downstream jet contain large turbulent eddies that remain coherent for long distances and are derived from the transitional vortices. However, these "coherent structures" in the turbulent jet differ significantly from the transitional vortices: for example, they are highly three-dimensional.

There is a small body of measurements of vortex passing frequencies and coalescence in the transition regions of cold jets as functions of the initial nozzle conditions. It is not difficult to envisage how the distinct physical events of

transition and the subsequent dominating large scale structure must have important repercussions where they occur in reacting jet flows, i.e., in turbulent diffusion flames. Some of the earliest studies² of vortex rings in jets were concerned with their effects on flame structure. However, investigations of the transitional flow of turbulent flames have not approached the thoroughness of investigations of cold flows. The major reason for this has been the lack of techniques capable of measuring quantities in flames with good temporal and spatial resolution. This paper describes the application of modern techniques to obtain data on combustion-flow interaction in a transitional jet flame with variation in nozzle conditions and comparisons between cold and burning jets. The relative "orderliness" of the transitional flow permits data to be interpreted to give both quantitative and qualitative information on the main physical phenomena resulting from combustion-flow interaction (mainly due to dilation and increased viscosity effects). In addition transitional flame structure is important in its own right, because of its occurrence in industrial practice and its influence on the turbulent flame further downstream.

Design and Philosophy of Experiment

Figure 1 shows the arrangement and notation for the jet flame experiment. The axisymmetric flame is produced by the flow of fuel gas through a 25.4 mm diam nozzle into a 400 m × 400 mm, low velocity (1 m/s), secondary air flow. The experiments are designed to derive time dependent information from measurements of fluctuating quantities in diffusion flames. A special effort is made in these experiments to measure, control carefully, and vary systematically, the flame initial and boundary conditions. Thus, measurements made in the flame eventually can be compared directly with modeling predictions based on these initial and boundary conditions. The burner nozzle is contoured to give a flat velocity profile at the exit with laminar internal and external boundary layers. The initial turbulence levels of both the primary (fuel jet) and secondary flows are low. Ignition and stabilization take place in a "cylindrical" laminar region near the nozzle lip. By progressively making measurements from the "simple" initial conditions at the nozzle, the natural development of the flame is followed, from the laminar conditions at the nozzle exit, through a transition region, to the fully turbulent flow downstream. This experimental forward marching procedure leads to a more fundamental understanding of the physical phenomena in the flame, particularly where an orderly "deterministic" structure exists.

Presented as Paper 80-0077 at the AIAA 18th Aerospace Sciences Meeting, Pasadena, Calif., Jan. 14-16, 1980; received Aug. 12, 1980; revision received Dec. 17, 1980. Copyright © American Institute of Aeronautics and Astronautics, Inc., 1980. All rights reserved.

*Research Fellow, Dept. of Chemical Engineering and Fuel Technology; now Lecturer, Dept. of Mechanical Engineering, UMIST, Manchester, England. Member AIAA.

†Reader, Dept. of Chemical Engineering and Fuel Technology. Associate Fellow AIAA.

‡Research Assistant, Dept. of Chemical Engineering and Fuel Technology.

§Research Student, Dept. of Chemical Engineering and Fuel Technology.

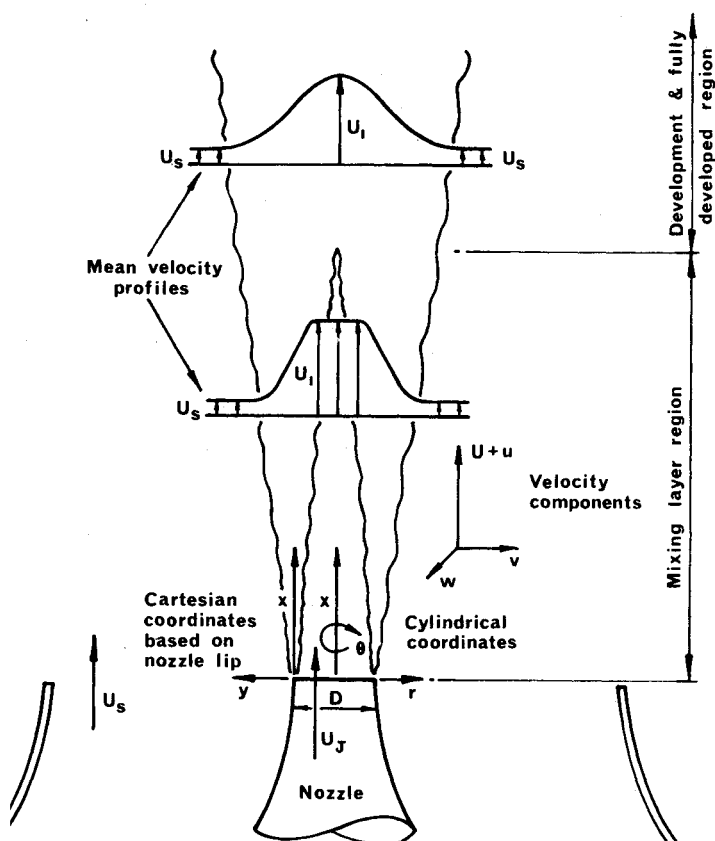


Fig. 1 Notation for round jet flame.

Important deterministic features of the flows described subsequently, such as burning interface layers, modes of instability of interfaces, reacting vortices, coherent large eddies, etc., are now being investigated by suitable measurement and data analysis techniques, particularly multiprobe conditional sampling.

Measurement Techniques

Laser Doppler Anemometry

Laser Doppler anemometry (LDA) was used to measure mean and fluctuating velocity. In these flows, which have velocities of the order of 10 m/s, the measurement control volume is $1 \times 0.15 \times 0.15$ mm and frequency response is of the order of 2 kHz (due to multiple scattering, not electronic, limitations). A forward scattering 1 W argon ion laser system is used with a counter processor interfaced with a DEC PDP11 computer. Cyclone seeders are used to supply SiO_2 seeding particles to both the jet and secondary flows. Tests, using a Bragg cell for frequency shifting, showed that reverse flows were not present in the flames. Thus LDA measurements were made without Bragg cells, to maximize the signal/noise ratios.

Fine Wire Thermocouples

A range of materials and diameters are used to construct fine wire thermocouples with digital compensation for convective and radiative heat transfer. A flat frequency response up to at least 2 kHz is achieved with 25 μm diam Pt-20%Rh/Pt-40%Rh wires.

Ionization Probe

Water cooled ionization probes are used to detect flame ionization and hence flame front location. These probes are similar to those used by Lockwood and Odidi.³

Laser Schlieren

The LDA system can be modified for use as a laser Schlieren system. A single, 1 mm diam laser beam is directed through the flame and strikes a micrometer "knife-edge." Density related refractive index changes deflect the beam and a photomultiplier records the resulting light intensity variations beyond the knife-edge. The photomultiplier output is thus dependent on the integral of transverse density gradients along the path of the laser beam.

High-Speed Cine Photography

A Hadland high-speed cine camera provides qualitative pictures of the flame structure and analysis of the films provides quantitative information of the dimensions, velocities, and passing frequencies of "events" in different regions of flames. The photographic information also provides a framework for the interpretation of fixed point measurements in terms of flame "structure," where such structure has recognizable organization. Most of the high-speed films have been taken using a color Schlieren system with 600 mm diam mirrors.

Experimental Results

The bulk of initial measurements have been made in a propane flame, jet flame I, with the following initial conditions: jet velocity, $U_J = 6.4$ m/s; Reynolds number, $Re = 10^4$; and propane/air equivalence ratio, $\phi = 10.4$. Measurements have been made in the first $20D$ of the flame. Measurements have also been made with variation in Re and ϕ . In all cases quoted values of the reference Reynolds number refer to cold conditions at the nozzle exit and the kinematic viscosity used is that of air. This is for reasons of simplicity and clarity and it is recognized that there are several other pertinent Reynolds numbers for the jet flames depending upon the properties of the propane/air mixtures and the reference temperature selected.

Cold Jet Structure: Hot Wire Data

Hot wire measurements have been made in cold air jets issuing from the burner nozzle. The hot wire, with its good spatial resolution and high frequency response, is used to specify the initial conditions of the flows, to provide velocity data for comparison and checking of LDA data, and to map the initial transitional cold jet in the frequency and spatial domains. The latter mapping provides information on the instabilities, vortex growth, coalescence, and vortex breakdown in the transitional cold jet for comparison with the jet flame. Unfortunately LDA techniques generally are not yet sufficiently developed to provide spectra in the jet flame with sufficient bandwidth to permit reliable comparison with hot wire spectra; instead, information on the frequency domain structure in the jet flame comes largely from other techniques.

The hot wire data are described in detail in a recent technical report⁴ and the main results are outlined here. Radial traverses at the nozzle for variation in Re , showed that the inner (high velocity side) nozzle boundary-layer thickness δ_j varied as $\delta_j/D = 9.5 Re^{-1/2}$ where δ_j is defined as $U_J(\delta U/\delta r)_{\max}^{-1}$. For cold jet 1, the nonburning "version" of jet flame 1 (with $Re = 10^4$) δ_j is 2.36 mm. The outer, lower velocity, boundary-layer thickness was $\delta_s \approx 4$ mm for all flows (except for certain flows with $U_s = 0$, studied for comparison). It was later found that flow structures in the flames are rather insensitive to the presence of the secondary flow. The secondary flow is necessary to give entrainment of seeding particles for the full length of the flame to permit accurate LDA measurements. Both the inner and outer nozzle boundary layers have laminar Blasius type profiles and the turbulence level at the nozzle exit plane was low with $(\bar{u}^2)^{1/2}/U_J < 0.005$.

For the cold jet, Michalke⁵ has used spatial and temporal stability theory to predict the growth of waves in the mixing

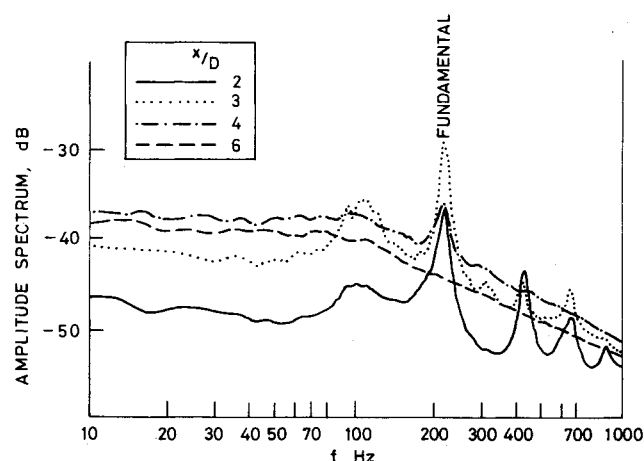


Fig. 2 Spectra of u in cold jet 1, $r/D = 0.5$, $Re = 10^4$.

layer near the nozzle. These are the Kelvin-Helmholtz instabilities. These waves are known to "roll up" into vortex rings. The most amplified frequency, predicted by Michalke, should correspond to the "natural" frequency of instability measured near the nozzle lip, provided that there are no strong external forcing pressure fields. To a first approximation this natural fundamental frequency of wave instability, or vortex shedding, has the proportionality $f_0 = 0.07 U_j / \delta_j$, so that the Strouhal number of the instability is approximately $f_0 D / U_j = 7.4 \times 10^3 Re^{-1/2}$ for the nozzle (cold flow). The full Michalke predictions show deviation from this simplified proportionality, and these results have been compared with hot wire frequency spectra measured near the nozzle for cold jets. The fundamental frequency derived from the peak in the measured spectrum near the nozzle lip, showed good agreement with Michalke's theory, typically within 5%. Figure 2 shows u spectra measured at different heights above the nozzle lip in the center of the mixing layer of cold jet 1. The fundamental frequency is at 215 Hz, while Michalke's analysis predicts $f_0 = 201$ Hz for the measured value of δ_j .

Figure 2 shows the appearance of harmonics and subharmonics in spectra, with increasing distance downstream. The harmonics are caused by high-frequency contributions from the viscous vortex cores, which develop in the center of the mixing layer. Harmonics are not found outside or at the edge of the mixing layer, where the cores have no direct influence. The subharmonic is caused by the coalescence of the vortex rings formed from the initial periodic instabilities, as has been described by Yule¹ and others. For this particular Re there is only one region of recognizable repetitive coalescence before turbulent flow is established at $x \approx 4.5D$, which is also, coincidentally, the length of the jet potential core region. The number of coalescing regions, the spectra, and the transition distance are all functions of Re , for a particular jet, as discussed by Yule.¹ The mean and rms velocity fields agreed well with previous experiments on cold round jets, and also with the LDA data, which are discussed later.

In summary, the hot wire measurements show that transition in the cold jet issuing from the burner nozzle, has the same general structure as that found in previous studies of jets issuing from near-laminar initial conditions. This structure includes a periodic initial instability, vortex growth, vortex coalescence, three-dimensional flow development, and the eventual establishment of turbulent flow with its broad spectrum of frequencies and an absence of spectral peaks inside the mixing layer region. The agreement between theory and experiment for the initial f_0 values shows that initial turbulence levels and external noise sources are sufficiently low to have no influence on the transitional flow.

A comparison of the flow structure with and without the secondary flow provided some interesting incidental ob-

servations. As expected, with $U_s = 0$ the jet spread a few percent faster than cold jet 1. In addition, there was evidence that the low velocity secondary flow had a small "stabilizing" influence on the transitional flow structure so that local fixed point periodic signals, caused by the vortices, exhibited less of the random amplitude modulation found for $U_s = 0$. However, there was no change in the length of the transition region between the jets with and without a secondary flow. Also, there was no difference between fundamental, harmonic, and subharmonic frequencies for the cases of $U_s = 0$ and $U_s = 1$ m/s. This demonstrates that these frequencies are determined by the inner nozzle boundary-layer profile, which is not influenced by the presence of the secondary flow.

Flow Visualizations of Flame

In an earlier paper, the authors⁶ have described direct observations of the flame based on flame luminosity. The occurrence of vortex motions, distorting the flame, and this coalescence of these vortices beyond $x = 16D$ was noted. However Schlieren films and point measurements have now revealed a flow structure that is considerably more complex than was first assumed. This complexity is caused by the simultaneous occurrence of several modes of instability near the nozzle so that more than one type of "coherent structure" can be observed at any one axial position. Flame luminosity indicates only a part of the structure and can thus be misleading. It has been found that the Kelvin-Helmholtz instabilities, which were at first assumed to dominate in the transitional flame, as in the cold jet described above, are accompanied by equally important combustion driven instabilities which are strongly influenced by the physicochemical properties of the fuel gas mixture.

Color Schlieren cine films have been made of flames with, in the first instance, systematic variation in equivalence ratio ϕ with Reynolds number Re fixed. Subsequently, Re was systematically varied while ϕ was maintained constant. This allows some separation of the effects of fluid mechanical and combustion mechanisms in the flame. The Reynolds number has been varied between 3×10^3 and 1.5×10^4 and ϕ has been varied between ∞ ("pure" diffusion flame) and 1.5 (i.e., approaching premixed conditions). In all of the flames studied vortex-like structures could be detected in at least the first $20D$ of flow. Significant changes can be observed when either ϕ or Re are varied.

Figures 3a-c are sketches derived from frames of the films and describe the typical appearance of the first $15D$ of jet flame I. The most obvious feature is a "double" structure with inner, fast moving eddies (convection velocity ≈ 6 m/s) and outer, large, slow moving eddies (convection velocity < 2 m/s). The inner eddies are hot/cold interfaces that have developed from wave instabilities of the initial cylindrical laminar interface. Most of the reaction in the transitional flame occurs at, or near, the interfaces. The interface waves coalesce and interact; wave amplitudes and wave lengths increase with distance downstream. The outer vortex-like eddies, which are also indicated by hot/cold interfaces, develop more slowly at first but they attain greater scales eventually. There appears to be no observable correlation or interaction between the outer and inner vortices up to about $x = 10D$. However, beyond this position, the outer eddies encroach increasingly into the center of the jet and there is obviously an interaction between the two instability modes. The outer hot flow region is termed a preheat zone and the inner interface is termed the reacting interface. The preheat zone, and indications of the interfaces, can also be seen in classical photographs of Wohl et al.⁷

With increasing distance downstream there is an increasing growth of "three-dimensionality." This is observed, first by vertical "streaks," and later by "cellular" interface structures, reminiscent of Schlieren photographs of turbulent premixed flames. Photographs taken by direct photography,⁶ using flame luminescence, show that the initial streamwise

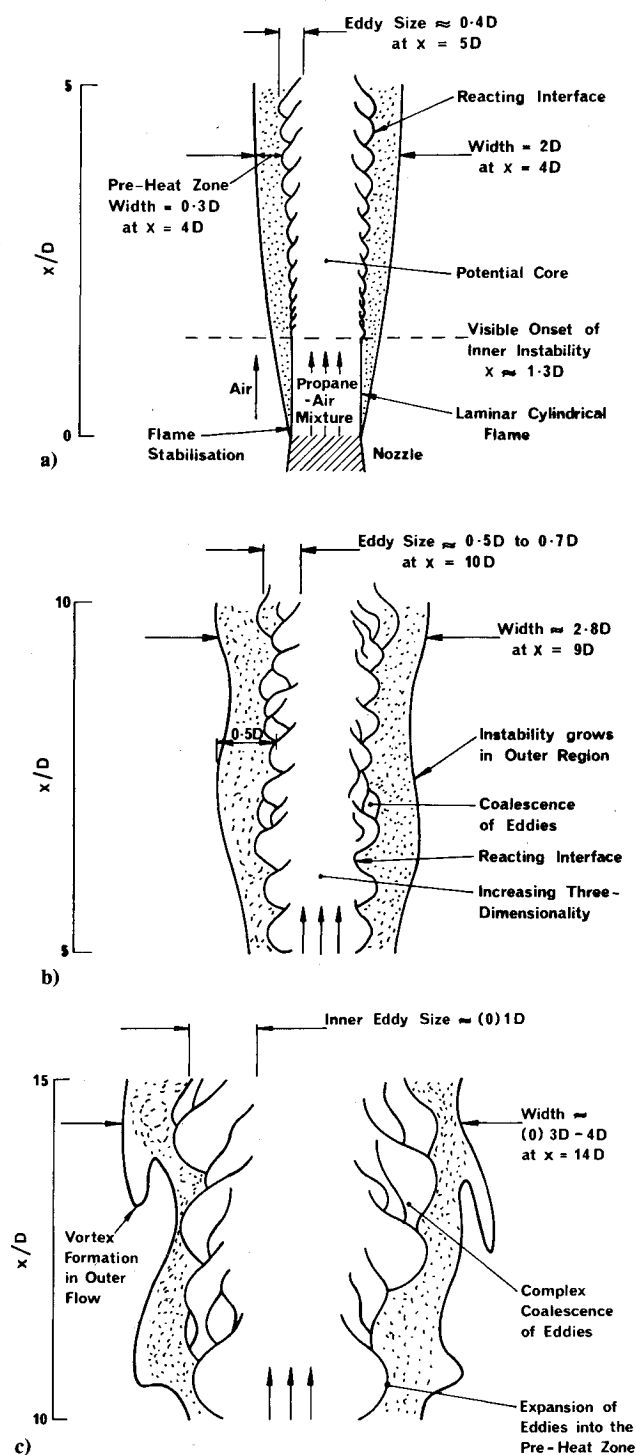


Fig. 3 Structure of jet flame 1: a) $0 < x/D < 5$, b) $5 < x/D < 10$, and c) $10 < x/D < 15$.

streaks are similar to those observed in cold jets¹ in which vortex rings develop azimuthal waves as one of the stages in the transition process. Films of flames with varying ϕ indicate that the local thickness of the preheat zone increases as ϕ decreases: as the jet mixture ratio is made leaner, the stoichiometric mixture "line" moves towards the jet center. Varying ϕ also changes the frequencies of the inner vortices, as discussed later in light of the laser-Schlieren measurements. Increasing Re resulted in higher vortex passing frequencies and the more rapid onset of three-dimensionality, and thus, presumably, a reduction in the transition length of the flame.

Interpretation of Schlieren films is hampered by the inability to interpret line-of-sight integrated data unambiguously in terms of point information. Further insight into

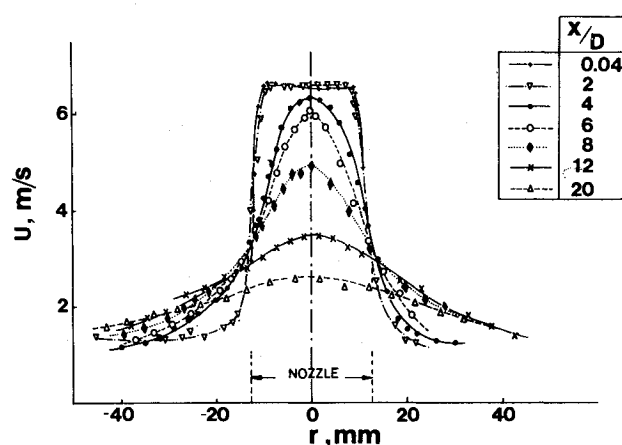


Fig. 4 Mean velocity distributions in cold jet 1, $Re = 10^4$.

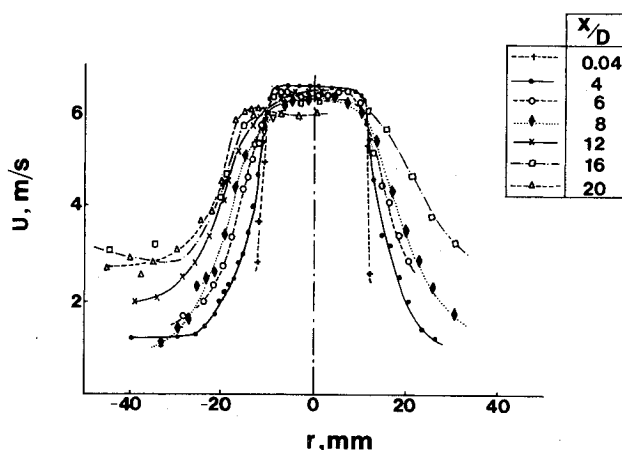


Fig. 5 Mean velocity distributions in jet flame 1, $Re = 10^4$, $\phi = 10.4$.

this interpretation problem can be gained by making use of the probe measurements and by filming the flow at the same time as measurements are made.

LDA Velocity Measurements

Figure 4 shows LDA measurements of mean velocity in cold jet 1. The data is in excellent agreement with hot wire measurements, and also with previously reported measurements, which indicates the good general accuracy of the LDA system.

Figure 5 shows mean velocity profiles in the first $20D$ of jet flame 1. These results are in dramatic contrast to the data, shown in Fig. 4, for the nonburning flow at the same Reynolds number. The potential core in the flame, as indicated by the central uniform velocity region, now apparently extends beyond $x = 20D$. The centerline velocity changes little in magnitude in the first $20D$ length of flame. Mean velocity gradients are generally higher in the flame than at the same axial position in the cold jet. However the total width of the flows do not differ greatly between the flame and cold cases, for any particular x value. Examination of individual velocity profiles in the flame reveals, at some stations, the occurrence of humps in the profiles, i.e., more than one inflexion point is found compared with the error function or Gaussian shapes in the cold jet. These humps were repeatable in the LDA measurements and they were not explicable by measurement uncertainties. These and other differences between the cold and burning flows need to be explained in terms of the various phenomena introduced by chemical reaction and heat release and how they interact with the orderly structure of the transitional flame.

Figures 6 and 7 show profiles of fluctuating velocity $(\bar{u}^2)^{1/2}/U_j$, measured by LDA in cold jet 1 and jet flame 1,

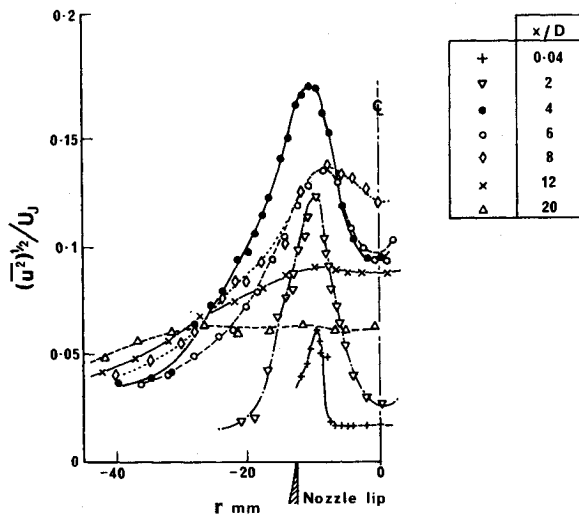


Fig. 6 Turbulence intensity distributions in cold jet 1.

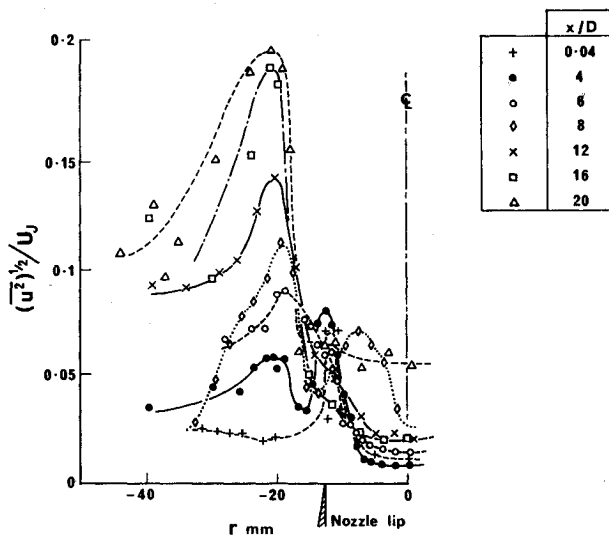


Fig. 7 Turbulence intensity distributions in jet flame 1.

respectively. A special experimental problem arises in measuring turbulence intensity in the mixing region very near the nozzle ($x=0.04 D$). LDA measurements in this region do not agree with hot wire data, which show turbulence levels less than 1% across the complete flow. The anomalous turbulence peak is produced by the spatial variation of particle velocities within the measurement volume here, which is relatively large compared with the shear layer thickness in this region.

In common with most published investigations using LDA, the LDA turbulence levels tended to be consistently higher than those measured by hot wires by approximately $U_j/100$. Thus a 1.5% turbulence level measured by LDA could correspond to 0.5% measured by hot wires. This overestimation of turbulence level by LDA is a result of an accumulation of the errors and biasing inherent in all LDA systems. Attempts are being made to further improve the signal processing and validation techniques. However, we are confident that data presented here are at least comparable in accuracy with the best of previously published LDA measurements in flames.

The turbulence distributions in Fig. 6 agree with previous results in cold round jets, using both hot wires and LDA. In this discussion the word turbulence is used for convenience but it should be emphasized that much of the flowfield investigated is of a transitional, rather than fully turbulent nature. Peak turbulence levels occur near the end of the potential core at $x \approx 4 D$ followed by a decay, approaching the rate x^{-1} required for exact similarity. The flame case, Fig. 7,

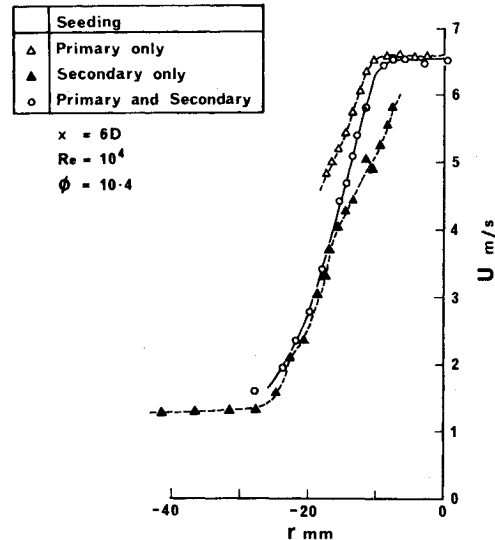


Fig. 8 Mean velocities measured in jet flame 1 with three types of LDA seeding.

is quite different, with a much slower increase in turbulence levels with increasing distance downstream, so that flame turbulence levels are lower than cold jet levels, at the same station, up to $x/D=10$. However the maximum levels in the flame at $x=20 D$, are higher than those found anywhere in the cold jet, i.e., 20% as opposed to 17%. Furthermore there is every likelihood of further increases beyond $x=20 D$, a region in which detailed measurements have not yet been made. The peak turbulence levels in the flame are found nearer to the outer, low velocity stream and the levels are low at the center of the mixing layer at the nozzle lip radius. Double peaks in the turbulence distributions are seen up to $x/D=6$ (Fig. 7). These are likely to be connected with the vortices or waves in the transitional flame and their interactions. These results show that there is a very significant influence of combustion on the velocity field in the initial region of the flame. Further work is required in order to explain these findings and develop models which are consistent with these phenomena.

In two-stream mixing flows, such as those investigated here, it is necessary to provide uniform seeding in both streams so as to avoid biasing effects in LDA measurements. The influence of changing seeding particle number density in each stream has not been reported in detail in the literature. Tests, which will be fully reported at a later date, were carried out in which the relative seeding densities of the primary and secondary flows were progressively varied. Very significant changes could be produced in both measured mean and, particularly, rms velocities, depending upon the relative seeding levels, and the position in the flow. This indicated the need for careful equalization of seeding levels before each set of experiments. Separate from this stratified-seeding problem, controlled changing of seeding levels can be usefully employed to derive conditionally sampled velocity data which can be interpreted in terms of intermittency and fuel/air mixing. Figure 8 shows an example, in which mean velocity profiles are measured with, 1) primary flow seeding only, 2) secondary flow seeding only, and 3) both flows seeded. The primary seeding velocity is higher than the local mean velocity, and the secondary seeding velocity is lower, which agrees with what could be expected from the analogous intermittency sampled data obtained in mixing layers in the past, by using hot wires. It is interesting to note that the primary flow (including the products resulting from burning of this primary flow) penetrates only to the center of the mixing layer. The secondary air penetrates the full width of the mixing layer up to the edge of the potential core. Mixing, and thus reaction, can only occur in the region of overlap of the two streams, i.e., approximately $7 \text{ mm} < r < 18 \text{ mm}$ at $x=6 D$.

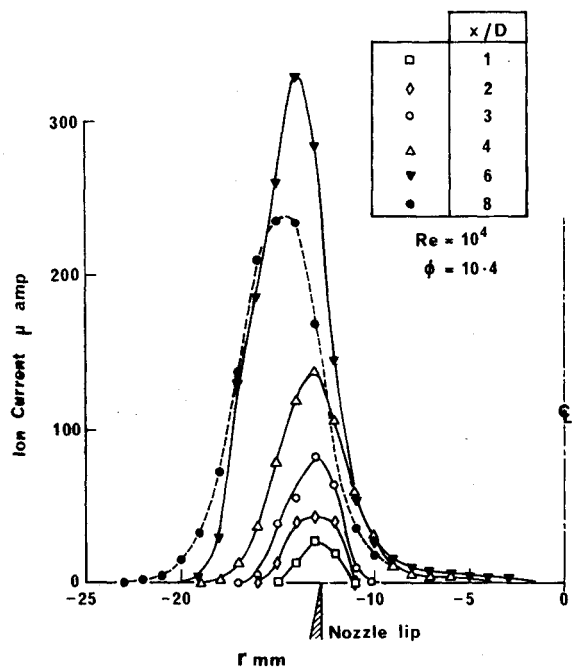


Fig. 9 Mean ionization probe signals in jet flame 1.

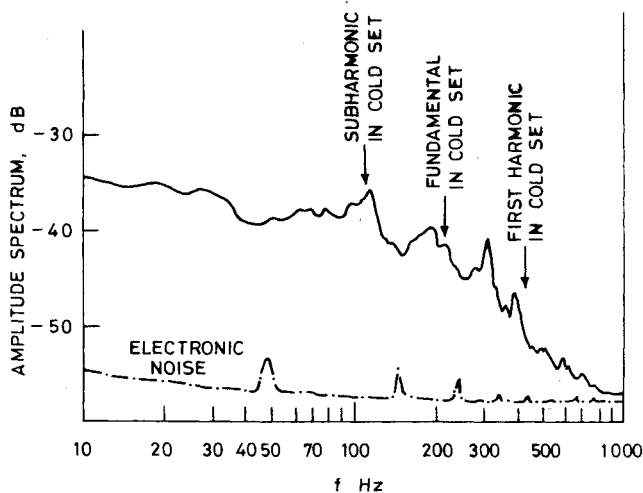


Fig. 10 Ionization probe spectrum in jet flame 1, $x/D = 8$, $r/D = 0.5$.

Ionization Level and Temperature

Measurements of ionization levels have been made in jet flame 1, including mean values, rms, pdf's, and frequency spectra. Problems of calibration drift, condensation, and sooting of the probe are encountered and these create particular difficulties with regard to the quantitative interpretation of fluctuating ionization density measurements. Distributions of mean ionization level are shown in Fig. 9. It is seen that the region of significant ion density is relatively narrow, compared with the total mixing-layer width indicated by the mean velocity distributions. High ionization levels indicate high rates of reaction at elevated temperatures. Comparison of Figs. 8 and 9 shows that the regions of overlap of the primary and secondary flow seeding particles (where mixing takes place) correspond with regions of high ionization levels. Peak signals are found near $x = 6 D$. Spectra have also been derived from ionization probe signals, e.g., Fig. 10. In certain flame regions these exhibit peaks which, as seen in Fig. 10, bear no clear relation with those found in the cold jet velocity spectra.

Temperature measurements have concentrated initially on a detailed mapping of the mean temperature field of jet flame 1 using fine wire thermocouples with digital processing and radiation corrections. Measurements of fluctuating temperature are currently in progress. Figure 11 shows mean temperature profiles in jet flame 1. The peak mean temperature is found near $x = 3 D$. The temperature peak moves progressively away from the center of the jet flame and, beyond $x = 3 D$, decays in value with increasing distance downstream. The peak temperature is always further from the jet center than the peak ionization level (cf. Figs. 9 and 11). The separation between the two peaks increases with increasing distance downstream. At each station, the total local mixing layer width, indicated by the mean temperature data, lies within 10% of the width indicated by the velocity profiles. It is known, from experiments in laminar premixed flames, that the region of highest gas temperature does not necessarily correspond exactly to the region of highest ionization level. However, this difference in position is small and cannot explain the large difference found between the positions of peak ionization level and peak mean temperature. In this region of the flame there appears to be an example of "counter-gradient diffusion" of heat, from the inner reaction zone, diffusing outward into a region of higher mean temperature. This is explained by the fluctuating nature of the inner reacting interface (see Fig. 3b), that results in a relatively low mean (not instantaneous) temperature, while the outer region has less fluctuations and thus a relatively high

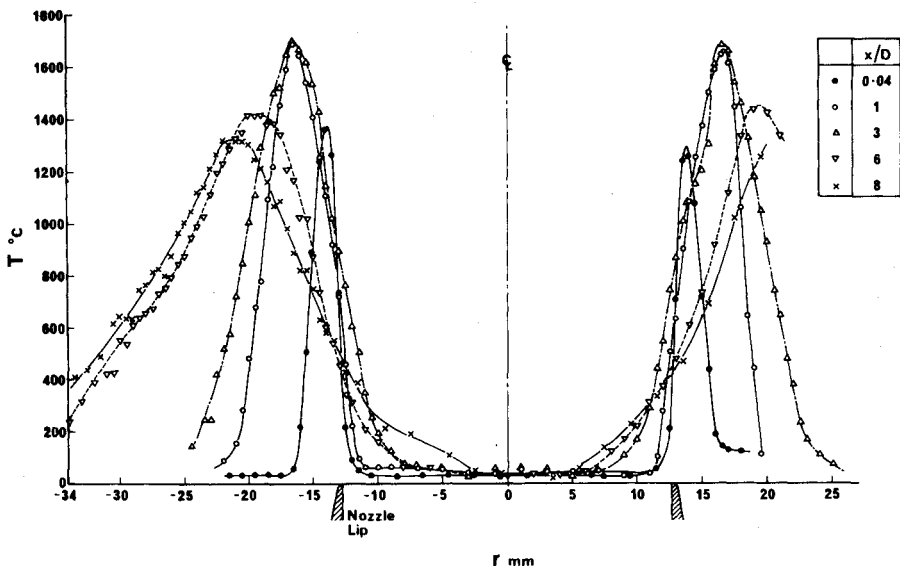


Fig. 11 Mean temperature distributions in jet flame 1.

mean temperature. This illustrates the pitfalls of the simpler phenomenological turbulence theories and shows the advantages of building up a clear physical model of the flame. The transitional flame lends itself well to the development of improved combustion models, because of its relative orderliness initially, and the subsequent building up of complexity with distance downstream.

Laser Schlieren Data

Figure 12 shows laser-Schlieren spectra measured at different longitudinal positions in jet flame 1, with the 1 mm diam laser beam passing through the flame, tangential to a cylindrical projection of the nozzle lip ($r = 0.5 D$). These spectra represent integrated data for the complete length of the beam, and they thus contain contributions from values of

r greater than $0.5 D$. The transformation of this integrated line of sight data, into "point" measurements is being investigated by using an Abel transformation (i.e., "tomography"). This utilizes spectra measured for several laser scans at different radial positions.

Figure 12 shows that distinct peaks are found which must result from the periodic wave and vortex structures seen in the Schlieren films. Several peaks are found at each axial station; in general, there is no clear harmonic relationship between all of the frequencies at which these peaks occur. Peak amplitudes of the distinct frequencies rise to maximum values at $x/D = 4$ and then decline with distance downstream. The peaks in the laser-Schlieren spectra occur at the same frequencies as the ionization probe spectra at the same position. Thus the density gradient fluctuations detected are caused by the passage of reacting interface layers. There is some general accord with the appearance of subharmonics of the initial Kelvin-Helmholtz instability in spectra in the transitional cold jet. However there are important and significant differences between the cold and flame cases; this is made clear by the results of a series of systematic experiments in which Re and ϕ were varied.

Figure 13 shows spectra obtained when Re was fixed and the equivalence ratio ϕ was varied. It can be seen that there is a gradual decrease in the most energetic frequency as ϕ is increased by increasing the proportion of fuel in the propane/air mixture, while maintaining a constant exit velocity. Similar trends were obtained at other Reynolds numbers. Figure 14 shows spectra obtained by maintaining a fixed equivalence ratio and varying the Reynolds number (i.e., varying the primary flow rate). It is seen that, for all Re , there are a series of distinct peaks in the spectra and the frequency values of these peaks are independent of Reynolds number. It is deduced that the inner vortices, which distort the initially laminar reacting layer (Fig. 3), cannot be simply explained as being due to Kelvin-Helmholtz instabilities, as generally found in cold jets, even if a first account is taken of the influence of heat release on diffusion coefficients and velocity profiles. Rather, it appears that additional combustion-driven instabilities are generated which result in wave and vortex structures similar in appearance to the Kelvin-Helmholtz vortices.

Thus there are a series of discrete frequencies at which the inner instability occurs and the values of these frequencies depend on the physio-chemical properties of the fuel gas. The flow rate (i.e., Re) determines the frequency, or batch of frequencies, from this series in which most of the energy is concentrated.

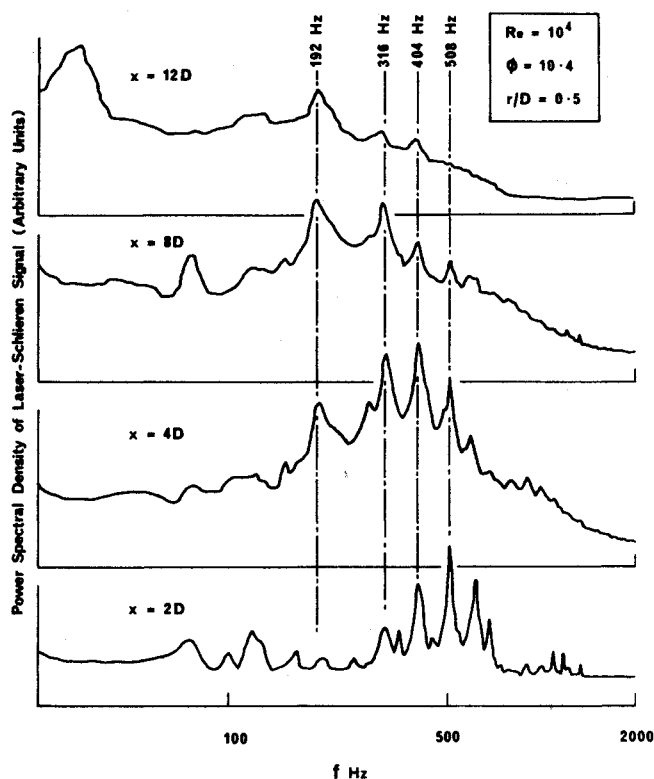


Fig. 12 Laser-Schlieren spectra in jet flame 1.

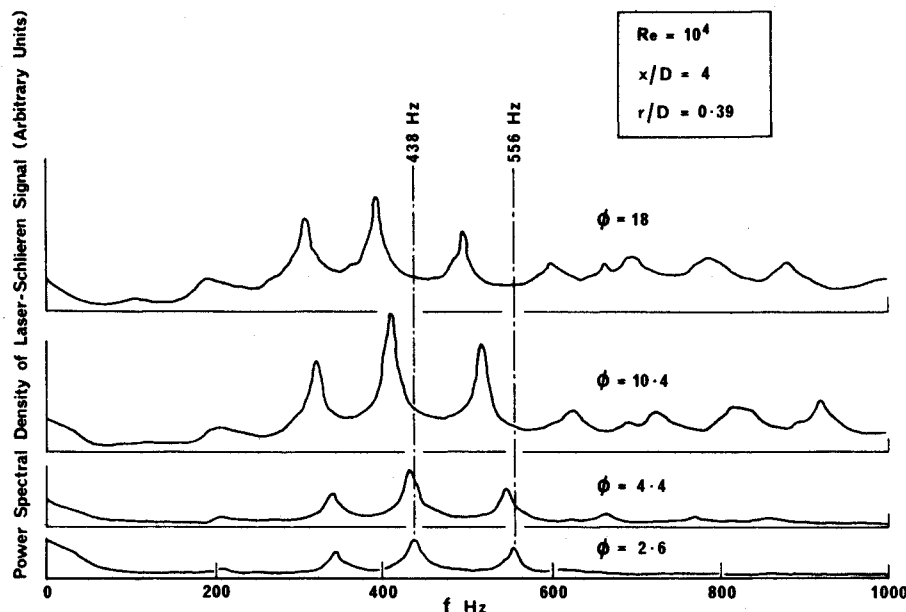


Fig. 13 Laser-Schlieren spectra, Re fixed, equivalence ratio varied.

Fig. 14 Laser-Schlieren spectra, equivalence ratio fixed, *Re* varied.

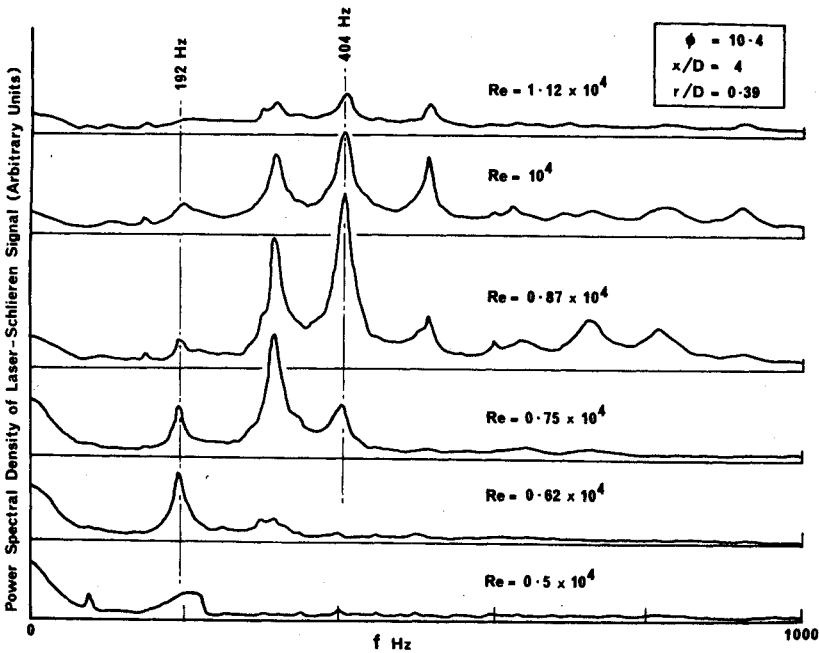


Fig. 15 Comparison of velocity, temperature, and ionization level profiles in jet flame 1.

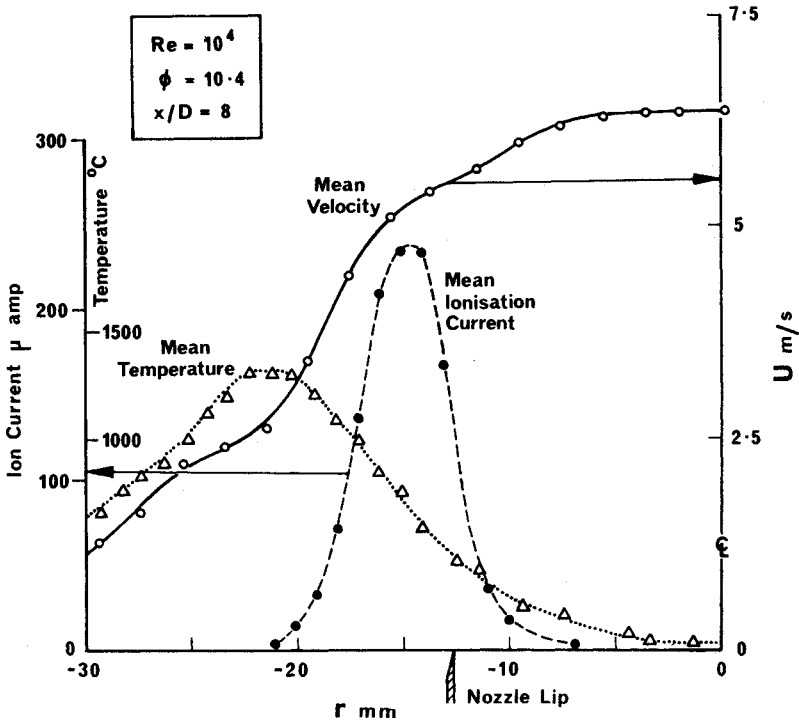
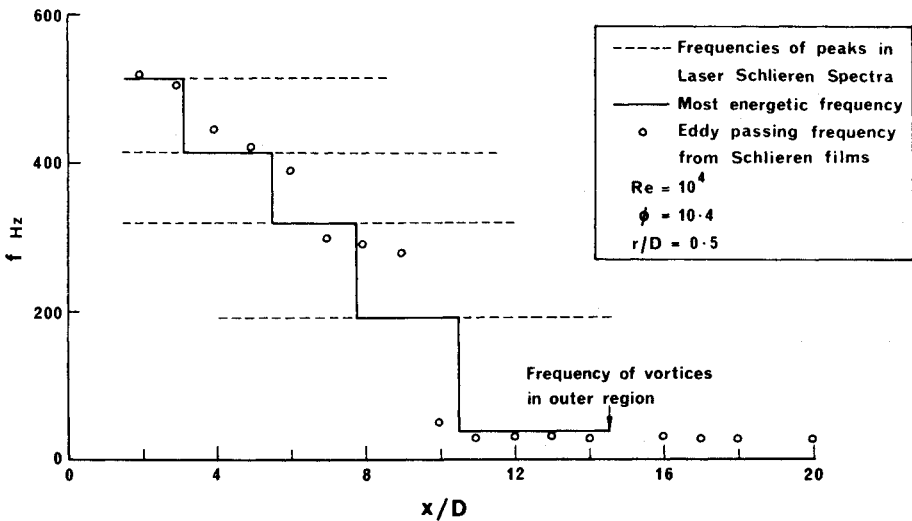


Fig. 16 Comparison of laser-Schlieren spectra peaks with eddy passing frequencies measured from cine films.



The simultaneous occurrence of some frequency peaks without clear harmonic relationships indicates that there may be more than one possible mode of instability occurring for any particular flame. There are several mechanisms and modes of combustion instability which have been proposed in the past, and further work is now in progress to determine the most important mechanisms in the present experiments. It should be noted that the initial conditions of the jet flame are essentially laminar and there were no indications, in the cold jets, of the peak frequency values found in the flames. Furthermore tests showed that the frequency spectra were insensitive to the application of an external sound field; this indicates that the initial instabilities result from a powerful mechanism which cannot easily be interfered with by the imposition of acoustic waves (due to fans, instruments, etc.).

Discussion and Concluding Remarks

LDA, thermocouple, and ionization probe measurements at $x = 8D$ in jet flame 1 are compared in Fig. 15. It is interesting to note that there is a hump in the mean velocity profile near the peak ionization level position. This can be explained as being due to flow acceleration accompanying reaction and heat release. One can also distinguish a hump in the velocity profile at the outer part of the flame that roughly corresponds to a region of high mean temperature.

The transitional flame structure is characterized by interacting waves and vortices which are responsible for the convolution of interfaces at which reaction is concentrated. These interfaces, on the inner side of jet flame 1, are clearly seen in Schlieren films and the passing frequencies of the eddies which they delineate, have been measured at different positions, as shown in Fig. 16. As these inner eddies move downstream, there is coalescence and growth in scale, while convection velocities do not change significantly. Thus the average passing frequency decreases with increasing distance downstream. Figure 16 also includes the frequencies at which peaks are found in the laser-Schlieren spectra. The solid lines denote the most energetic frequency peaks; the broken lines indicate the other frequency peaks found at a given axial position. The agreement between the most energetic peaks and the frequencies measured from the films is seen to be good. Thus the vortices seen on the inner side of the mixing layer are responsible for the spectral peaks. Analysis of cine films requires subjective judgment, at times, and there is inevitably a "smearing out" of the coalescing, or other processes, responsible for the transfer of energy between discrete frequencies. Beyond $x = 10D$, the dominant frequency is near 30 Hz, and this is considered to correspond with the encroachment of the large, slow moving, outer vortices, across most of the width of the mixing layer.

In conclusion, the initial region of a flame has a similar general structure for a wide range of Reynolds numbers and equivalence ratios. This involves combustion driven instabilities on the inner side of the flame that results in wave and vortex deformations of the reaction zone. Separate instabilities develop at the outer part of the flame. The initial region consists of a wrinkled two-dimensional laminar flame. However, the coalescing and interaction between adjacent waves and vortices, interaction between instability modes, and the gradual development of three-dimensional flow results in the more complex turbulent flame structure. However, sections of reacting interface, initially laminar near the nozzle, can be tracked visually as they move downstream, up to the turbulent flame region and beyond. Although the existence of vortices is common to the flame and cold jet cases, as are coalescing and three-dimensional growth via azimuthal waves, the two cases are very different quantitatively. The most obvious differences are the lengthening of the jet potential core for the flame case and the damping of the initial eddy growth, but eventually achieving higher turbulence levels, in the flame.

Acknowledgments

Research in the area of coherent structures in turbulent flames is supported at Sheffield, by the U.S. Office of Naval Research (Project SQUID), Subcontract 8960-30 and the Air Force Office of Scientific Research/AFSC, United States Air Force under Grant AFOSR-77-3414.

References

- ¹Yule, A. J., "Large Scale Structure in the Mixing Layer of a Round Jet," *Journal of Fluid Mechanics*, Vol. 89, Pt. 3, 1978, pp. 413-432.
- ²Tyndall, J., "On the Action of Sonorous Vibrations on Gaseous and Liquid Jets," *Philosophical Magazine*, London, Vol. 4, Pt. 33, 1967, pp. 375-391.
- ³Lockwood, F. C. and Odidi, A.O.O., "Measurement of Mean and Fluctuating Temperature and of Ion Concentration in Round Free Jet Turbulent Diffusion and Premixed Flames," *Fifteenth Symposium (International) on Combustion*, Combustion Institute, Pittsburgh, Pa., 1975, pp. 561-571.
- ⁴Chigier, N. A. and Yule, A. J., "The Structure of Eddies in Turbulent Flames—I," Technical Rept., Project SQUID, Purdue University, March 1979.
- ⁵Michalke, A., "Vortex Formation in a Free Boundary Layer According to Stability Theory," *Journal of Fluid Mechanics*, Vol. 22, Pt. 2, 1965, pp. 371-383.
- ⁶Chigier, N. A. and Yule, A. J., "The Physical Structure of Turbulent Flames," AIAA Paper 79-0217, New York, Jan. 1979.
- ⁷Wohl, K., Gazley, C., and Kapp, N., "Diffusion Flames," *Third Symposium on Combustion and Flame and Combustion Phenomena*, Combustion Institute, Pittsburgh, Pa., 1949, pp. 288-300.